ENCLOSURE 3

Ziada, S. & Buhlman, E. T., 1992 Self-Excited Resonances of Two Side Branches in Close Proximity. Journal of Fluids and Structures 6, 583-601.

Journal of Fluids and Structures (1992) **6**, 583–601

SELF-EXCITED RESONANCES OF TWO SIDE-BRANCHES IN CLOSE PROXIMITY

S. ZIADA AND E. T. BÜHLMANN†
Laboratory for Vibrations and Acoustics, Sulzer Brothers Ltd, Winterthur, Switzerland

(Received 3 September 1990 and in revised form 16 July 1991)

Complex piping systems with multiple side-branches in close proximity are very liable to flow-induced acoustic resonances. This is demonstrated by means of model tests of two piping systems, one with a single side-branch the second containing two side-branches. The general acoustic response of these two systems is studied as the flow velocity in the main pipe is increased. The influence of the distance between the branches, the branch length, the static pressure, the upstream turbulence level and the angle between the branches is also investigated.

1. INTRODUCTION

ACOUSTIC RESONANCES OF BRANCH PIPES are often strongly excited by the flow over the mouth of the branch. The resonance modes consist of odd multiples of a quarter wavelength along the branch pipe [see Figure 1(a)]. When a resonance occurs, the amplitude of the acoustic pressure pulsation can be several times higher than the dynamic head in the main pipe. This level is sufficiently high to cause severe noise and vibration problems in a wide variety of engineering applications [see, for example, Chen & Florjancic (1975), Chen & Stuerchler (1977), Coffman & Bernstein (1980), Chen & Ziada (1982), Baldwin & Simmons (1986) and Bernstein & Bloomfield (1989)].

The excitation mechanism of branch pipe resonances is similar to that causing acoustic resonances of deep cavities exposed to grazing flow. The latter case has received considerable attention in the literature, due to its importance in aeronautical and marine applications. Deep cavity oscillations have been investigated by East (1966), De Metz & Farabee (1977), Elder (1978), Elder *et al.* (1982), Parthasarathy *et al.* (1985) and others. Rockwell & Naudascher (1978) and Rockwell (1979, 1983) have reviewed the oscillation mechanisms of flow past deep and shallow cavities.

Flow-induced resonances of deep cavities and branch pipes are classified by Rockwell & Naudascher (1978) as fluid-resonant oscillations. These oscillations are self-sustained due to the coupling between the resonant acoustic field and the unstable shear layer which spans the mouth of the cavity. At the point of separation, the acoustic field induces velocity fluctuations in the shear layer. If the shear layer is unstable at the frequency of the acoustic field, it extracts energy from the mean flow to amplify the initial velocity fluctuations into large scale vortex-like structures. Further downstream, the interaction of the formed vortices with the acoustic field and the cavity downstream corner transfers the fluctuating energy of the shear layer back into the resonant acoustic field. This last event of the excitation mechanism is the most difficult to characterize. Considerable insight, however, has been provided in recent work by Welsh and his co-workers (Hourigan *et al.* 1986, 1990; Stoneman *et al.* 1988).

† Present address: Ransburg-GEMA, St Gallen, Switzerland.

0889-9746/92/050583 + 19 $03.00

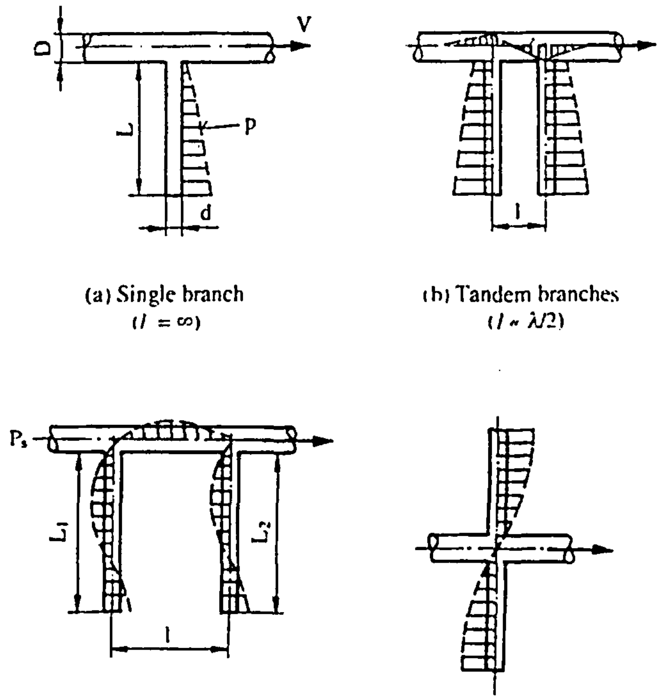

(a) Single branch ($l = \infty$)

(b) Tandem branches ($l \approx \lambda/2$)

(c) Tandem branches ($l \approx \lambda/2$)

(d) Co-axial branches ($l = 0$)

Figure 1. Typical geometries of side-branches and simplified patterns of acoustic pressure distributions in the branches.

They used Howe's theory of aerodynamic sound (Howe 1975) to show that acoustic energy can either be generated or absorbed by vortices convecting within a fluctuating acoustic field. They were able to explain, by means of experiments and numerical simulations, why resonances occur over certain ranges of Strouhal number and why each range is characterized by the number of the vortices formed in the shear layer.

Although the excitation mechanisms for branch pipes and deep cavities in moving vehicles are basically similar, there are important geometrical and flow differences which preclude the applicability of the well documented data on cavity flow to industrial cases of branch pipes. Pipe flow past a branch is usually very turbulent, which is not the case in most of the cavity investigations. Moreover, the ratio between the branch and the main pipe diameters (d/D)† is crucial in determining the pressure amplitude and, to a lesser extent, the Strouhal number of resonance (Jungowski *et al.* 1989). Finally, the acoustic characteristics of the associated piping system must also be taken into account where branch pipes are concerned.

There is a paucity of published work on pipe branches other than case histories. Jungowski *et al.* (1989) reported a substantial reduction in the pulsation amplitude when the diameter ratio (d/D) was increased. Erickson *et al.* (1986) observed resonances at two different ranges of Strouhal number. Flow visualization of the shear layer revealed the formation of either a single vortex, during the lower Strouhal number resonance, or two vortices, during the higher Strouhal number resonance. The pulsation amplitude was substantially higher for the single vortex case.

† A list of symbols is given in the Appendix.

Bruggeman (1987) investigated the case of two side-branches separated by a distance approximating half the wavelength of the resonant acoustic field. He addressed, among other aspects, the effect of the static pressure on the acoustic damping due to friction losses, and suggested a limit amplitude of pulsation when friction losses become negligible at high pressures.

The present investigation focuses on piping systems involving two branches in close proximity. It was motivated by field experiences which indicated that multiple branches are much more liable to flow-induced vibration than single branches. The first results of a research project initiated to investigate this phenomenon are presented in this paper. Attention will be focused on the *general characteristics* of the system acoustic response.

The cases which are of primary interest are shown in Figure 1. They are classified according to the distance, l, between the branches. This distance is much smaller than one half of the acoustic wavelength in case (b), approximates one half of the wavelength in case (c) and is zero in case (d). Since case (c) has been investigated in detail by Bruggeman (1987) and Bruggeman *et al.* (1989), it will not be considered here in any detail. Only cases (b) and (d) are investigated and compared with the case of a single branch, i.e. case (a). Several counter-measures which can be adopted to eliminate the observed resonances are also addressed.

2. SINGLE VERSUS MULTIPLE SIDE-BRANCHES

Figure 2 shows schematically the pattern of the acoustic flux at the resonance of three different systems of side-branches. In the single branch case, Figure 2(a), the amplitude of the pressure pulsation in the branch is influenced by, among other parameters, the acoustic radiation from the branch into the main pipe and subsequently, by the friction and heat losses in the main pipe as well as by the radiation losses at the main pipe terminations. These effects can be clearly demonstrated by considering the recent results on single branches reported by Jungowski *et al.* (1989). The pressure amplitude at resonance reported by these authors is plotted in Figure 3 as a function of the diameter ratio, d/D. The Mach number is constant for each curve. It is seen that increasing the ratio d/D, which increases the radiation losses into the main pipe, is associated with a rapid reduction in the pulsation amplitude at resonance. The effect of the boundary conditions at the main pipe terminations is also illustrated in Figure 3.

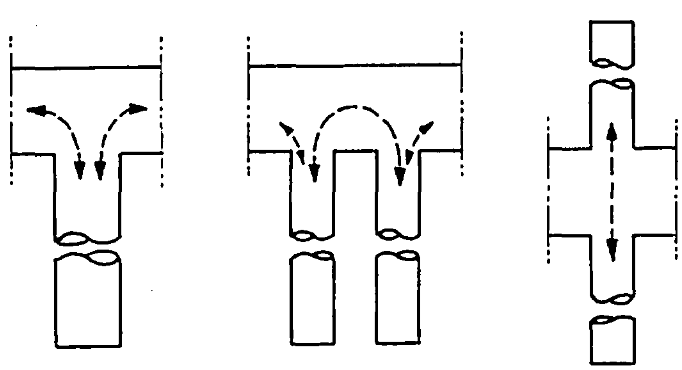

(a) (b) (c)

Figure 2. Schematic presentation of the acoustic flux in side-branches: (a) single branch; (b) tandem branches; (c) co-axial branches.

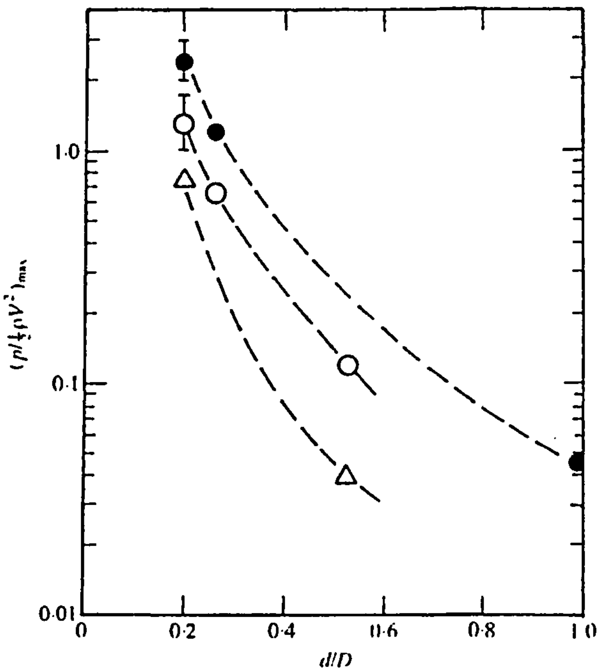

Figure 3. Effect of the diameter ratio on the maximum pressure amplitude generated at the first mode resonance of single branches for $r/d = 0$: △, $M = 0 \cdot 1$; ○, ●, $M = 0 \cdot 15$. ●, Reflective endings: △, ○, non reflective endings. All data from Jungowski *et al.* (1989).

The pulsation amplitude increases when reflective terminations are used to reduce the radiation losses.

In the case of two branches, which are well tuned and in close proximity, Figure 2(b, c), the acoustic flux at the mouth of one branch is equal but opposite to that at the mouth of the other branch. *The two branches therefore strongly couple and form a subsystem with negligible radiation losses.* Due to this reduction in the radiation damping, the pulsation amplitude in the case of two (or multiple) branches can be substantially higher than that in the case of a single branch. As will be shown in the present paper, the difference between the acoustic response of single and multiple side-branches under similar test conditions can be drastic for large values of d/D. Thus, while a single side-branch with a ratio of $d/D = 1 \cdot 0$ and under certain boundary conditions may be regarded as harmless with respect to vibrations, see Figure 3, a two-branch system with the same diameter ratio and under the same boundary conditions can cause serious vibration problems.

3. EXPERIMENTAL FACILITY

A pressurized air test facility was used to carry out the tests. It has a maximum capacity of about 0·6 kg/s and a maximum supply pressure of 5 bar. All pipes, including the branches, were made of steel. As shown in Figure 4, the facility is equipped with a filter, a low-noise pressure regulator, two dissipative silencers (one upstream and another downstream of the test section) and a metering orifice plate. The use of the dissipative silencers at both ends of the test section made the main pipe less reactive and, therefore, reduced the effect of the main pipe acoustics and of the boundary conditions on the acoustical response of the branches.

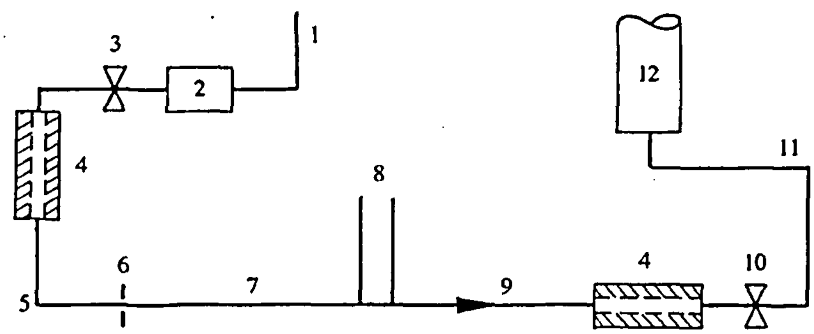

Figure 4. Schematic presentation of the test rig. The numbers denote: 1, pressurized air supply; 2, filter; 3, low noise pressure regulator; 4, absorption silencer; 5, pipe (3·1 m); 6, metering orifice; 7, upstream pipe (5·05 m); 8, side branches; 9, downstream pipe (1·7 m); 10, throttle valve; 11, high pressure hose; 12, exhaust chimney.

The tested geometries represented models of piping systems commonly used in power plants, such as the piping systems of turbine by-pass valves and safety relief valves. The inner diameter of the main pipe was $D = 89$ mm. The other test parameters (see Figure 1 and the list of symbols) were: $d/D = 0{\cdot}57$; $l/d = 2{\cdot}35 - 5{\cdot}6$; $L = 0{\cdot}61 - 2{\cdot}0$ m; $R < 4 \times 10^5$ and $M < 0{\cdot}15$. The T-joints of the branches had sharp edges. Unless otherwise stated, all the tests were carried out with two branches of equal length, i.e. $L_1 = L_2 = L$, see Figure 1.

The first set of experiments was conducted at atmospheric pressure. In this case, the downstream silencer was connected directly to the exhaust chimney by means of a high pressure hose. At a later stage, the system was pressurized by installing a throttle valve at the downstream end, see Figure 4. Thus, it was possible to vary the static pressure during the tests.

During the atmospheric pressure tests, the pressure pulsations in the main pipe and at the closed end of the branches were monitored by means of Brüel and Kjaer $\frac{1}{4}''$ microphones. These were replaced by Kistler pressure transducers when the system was pressurized. All transducers were flush-mounted to the inner wall of the pipes. Spectral analysis of the pressure signals was carried out by means of a Nicolet 444A spectrum analyser. In some cases, a two-channel Hewlett Packard analyser was used to measure the phase between the pressure pulsations at the closed ends of the branches.

4. TEST RESULTS

4.1. General System Response

4.1.1. *Two branches in tandem*

The geometry of two branches arranged in tandem, as shown in Figure 1(b), was tested first. The pressure pulsations were measured at the closed end of the two branches, as the flow velocity, V, in the main pipe was increased in steps. In all the tests reported upon here, the pressure pulsation in the downstream branch was about 10% smaller than that in the upstream branch. The cause of this slight, but consistent, difference is not known and has not been investigated to date. All the results given hereafter were taken at the end of the upstream branch.

Figure 5 shows the development of the pressure spectra as the mean flow velocity in the main pipe was increased from 10 to 86 m/s. The spectral peaks indicate the occurrence of resonances at the frequencies of the acoustic modes. These frequencies

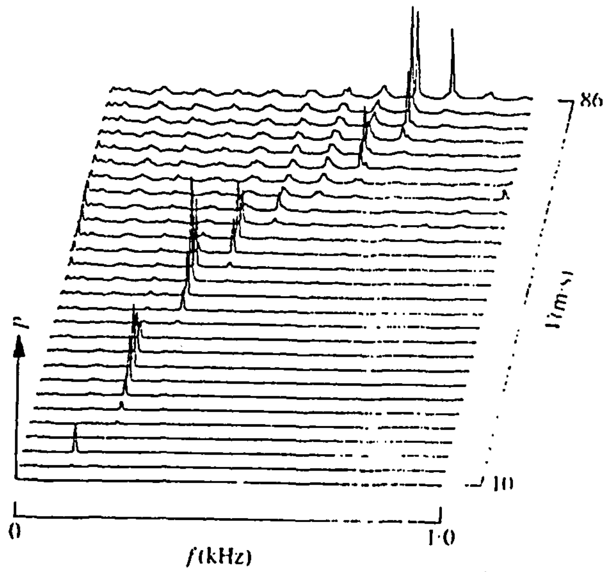

Figure 5. Development of the pressure spectrum measured at the closed end of the upstream branch as the flow velocity is increased; $L_1 = L_2 = 2$ m, $l/d = 2{\cdot}35$, $P_s = 0{\cdot}96$ bar.

can be estimated from

$$f_n = \frac{(2n-1)C}{4[L + (l/2)]}, \qquad n = 1, 2, 3, \ldots \tag{1}$$

where C is the speed of sound and n is the acoustic mode order (not related to the shear-layer mode). The difference between the measured frequencies and those calculated from equation (1) was less than 5%.

It is noteworthy that the results given in Figure 5 correspond to cases (b) and (c) of Figure 1. At low velocities, the wavelength of the excited (lower) modes is much larger than the distance between the two branches, i.e. $l \ll \lambda/2$. In this case, the pressure pulsations at the ends of the branches should be out of phase. This is seen to be the case in Figure 6(a), which shows the signals of the pressure pulsations at the closed ends of the branches during the resonance of the third mode. The phase between the two signals is 174·8°. At high velocities, the frequencies of the excited (higher) modes

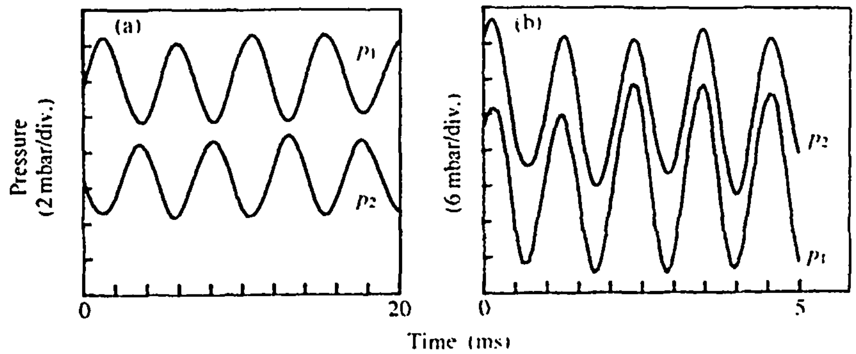

Figure 6. Signals of pressure fluctuations at the closed ends of the tandem branches during (a) third mode resonance ($f_3 = 212$ Hz) and (b) eleventh mode resonance ($f_{11} = 896$ Hz); $L = 2{\cdot}0$ m, $l/d = 2{\cdot}35$, $P_s = 0{\cdot}96$ bar.

are so high that one half of the acoustic wavelength becomes comparable with the distance l. As shown in Figure 6(b), the pressure pulsations at the ends of the branches during the resonance of the eleventh mode are virtually in-phase (the phase difference is 11°). Note that there is an intermediate velocity range in Figure 5 within which the acoustic modes were only weakly excited. This is because the wavelength corresponding to these modes is neither much smaller than nor comparable with $\lambda/2$.

The frequency, f, the r.m.s. amplitude, p, and the Strouhal number, S, of the dominant pressure pulsations are given in Figure 7 as functions of the flow velocity.

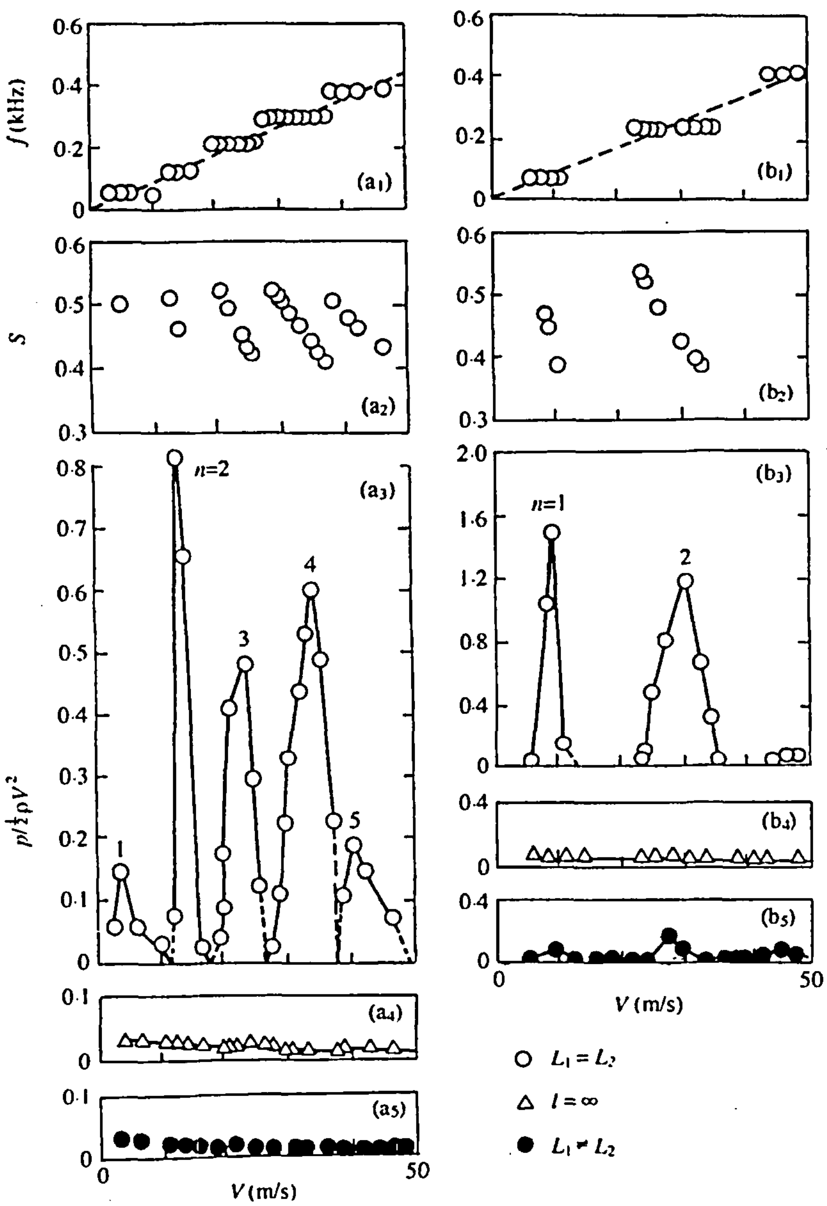

Figure 7. General response of two branches in tandem in comparison with those of a single branch and detuned tandem branches: (a_1), (a_2), (a_3), tandem branches, $L = 2{\cdot}0$ m, $l/d = 2{\cdot}35$; (b_1), (b_2), (b_3), tandem branches, $L = 1{\cdot}0$ m, $l/d = 2{\cdot}75$; (a_4), (b_4), single branch; (a_5), (b_5) detuned branches, $\Delta L/L_1 = 15\%$. $P_s = 0{\cdot}96$ bar.

Two cases are given; $L_1 = L_2 = 2{\cdot}0$ m and 1·0 m. The r.m.s. amplitude is nondimensionalized by the dynamic head in the main pipe. The data given in the Strouhal number plots correspond to the pulsation amplitudes which exceeded about 10% of the dynamic head.

As can be seen from Figure 7, higher order modes are consecutively excited as the flow velocity is increased. The broken lines shown in Figure 7(a_1, b_1) are drawn through the data points of maximum pulsation amplitude. They yield a Strouhal number of $S = fd/V = 0{\cdot}45$, which agrees very well with the value reported by Jungowski *et al.* (1989) for a single branch with a diameter ratio of 0·52.

It should be noted, however, that the occurrence of large amplitude pressure pulsations is not associated with a single value of S, but rather with a certain range, as shown in Figure 3(a_2, b_2); this range depends on the static pressure inside the pipe. Tests with higher pressures resulted in a resonance range of $S = 0{\cdot}27$ to 0·55. *A lower bound of $S = 0{\cdot}55$ is therefore recommended for design purposes.* This value gives the maximum allowable flow velocity consistent with the avoidance of resonance.

The amplitude of the pressure pulsations for the case of a single branch was also measured under the same test conditions and is given in Figure 7(a_4, b_4). It does not exceed 10% of the dynamic head, which agrees with the results of Jungowski *et al.* (1989). The presence of the second branch is seen to increase the resonance amplitudes by more than one order of magnitude. These findings suggest that the results obtained from tests on single branches, particularly these with large diameter ratio, are not necessarily applicable to cases involving two branches.

4.1.2. *Co-axial branches*

The acoustic response of co-axial branches at atmospheric pressure is shown in Figure 8. The measured resonance frequencies which are given in the figure agree, to within 5%, with the prediction of equation (1) after replacing the dimension l by the diameter of the main pipe. The overall system response is similar to that of the tandem branches discussed earlier, except that the dimensionless amplitude is higher and the lock-in range is wider for the case of co-axial branches. These findings are logical, since the radiation damping of the co-axial branches is smaller than that of two branches in tandem, see Figure 2(b, c). In spite of this increase in the lock-in range and the pulsation amplitude, the Strouhal number of large amplitude pulsation did not exceed the recommended design value of 0·55.

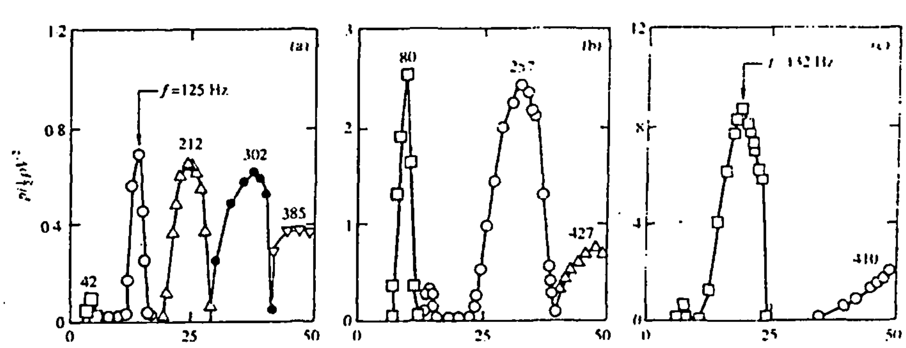

Figure 8. General response of the co-axial branches: (a) $L_1 = L_2 = L = 2{\cdot}0$ m; (b) 1·0 m; (c) 0·61. m. □, mode 1; ○, mode 2; △, mode 3; ●, mode 4; ▽, mode 5. $P_s = 0{\cdot}96$ bar.

It is noteworthy that the resonance amplitude in Figure 8(c) is about one order of magnitude higher than the dynamic head in the main pipe. This underscores the damage potential of acoustic resonances in piping systems with multiple branches.

The overall responses of the tandem and of the co-axial side-branches, Figures 7 and 8, have several additional features in common. First, there seems to be a minimum Reynolds number, or dynamic head, which is required to excite the resonance, i.e. to achieve the lock-in phenomenon. This can be seen in Figures 7(a_3) and 8(a), which show a very weak response of the first mode. The second feature concerns the higher order modes. When the minimum Reynolds number is exceeded, the *dimensionless* amplitude at the resonance of the higher order modes decreases as the mode order (n) is increased. This agrees with the results of single branches reported by Jungowski *et al.* (1989). The higher modes, however, have a wider range of lock-in. In other words, the range of the Strouhal number within which large amplitude pulsations occur is wider for the higher modes. Finally, it should be noted that increasing the frequency of any mode, by shortening the branches, results in an increase in the dimensionless amplitude at resonance. This feature is particularly apparent in Figure 8. Jungowski *et al.* (1989) reported similar results for single branches.

4.2. Effect of the Distance Between the Branches

The effect of the distance between the tandem branches is shown in Figure 9 for the case $L = 1{\cdot}0$ m. The response amplitude of the first two modes is seen to decrease as the ratio l/d is increased. At $l/d = 5{\cdot}6$, for example, the dimensionless amplitude becomes one order of magnitude smaller than that occurring at $l/d = 2{\cdot}35$. Another

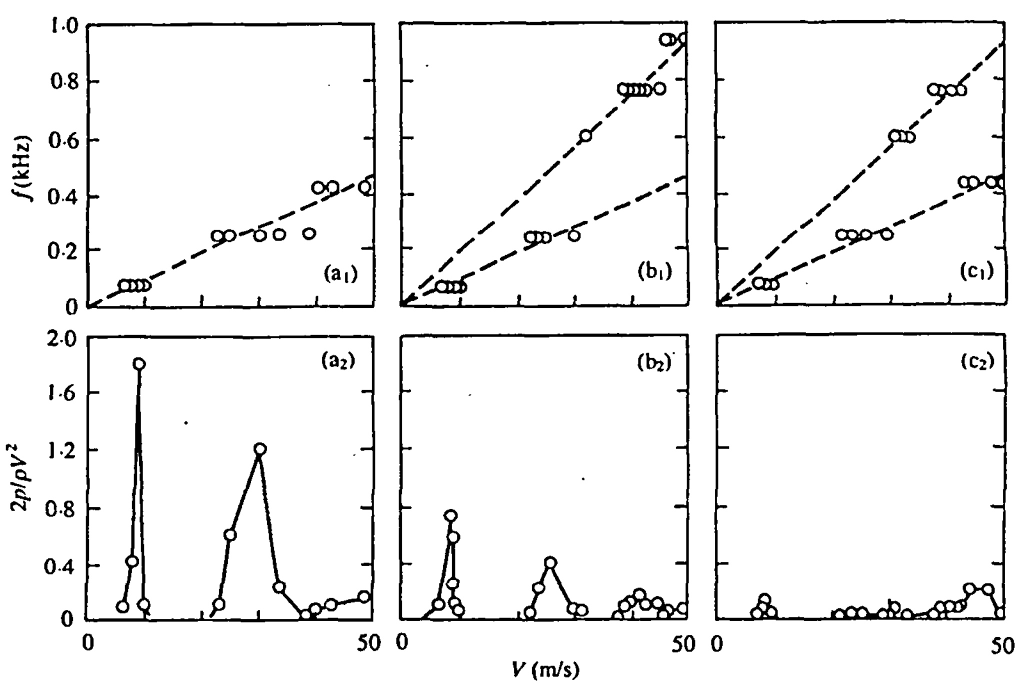

Figure 9. Frequency and amplitude of the pressure pulsation as functions of the flow velocity for three values of the spacing between the tandem branches: (a) $l/d = 2{\cdot}35$; (b) $l/d = 4{\cdot}3$; (c) $l/d = 5{\cdot}6$. $L = 1{\cdot}0$ m, $P_s = 0{\cdot}96$ bar.

result of increasing the ratio l/d is the increased liability of the higher modes to excitation. As shown in Figure 9(b_1, c_1), the resonance Strouhal number of the higher modes is about *twice* that of the lower modes. The resonance amplitude, however, is relatively small.

As mentioned in the Introduction, the occurrence of resonance at twice the main Strouhal number has been observed for single branches as well. It is associated with the formation of two vortices in the shear layer (Erickson *et al.* 1986). The pulsation amplitude resulting from this shear-layer mode is much weaker than that produced at the main Strouhal number (Jungowski *et al.* 1989). These features of the single branch case agree with the present results for two branches.

Figure 10 depicts the maximum dimensionless amplitude measured at the resonance of each mode as a function of the ratio l/d. The amplitude is seen to become very small for sufficiently large values of the ratio l/d.

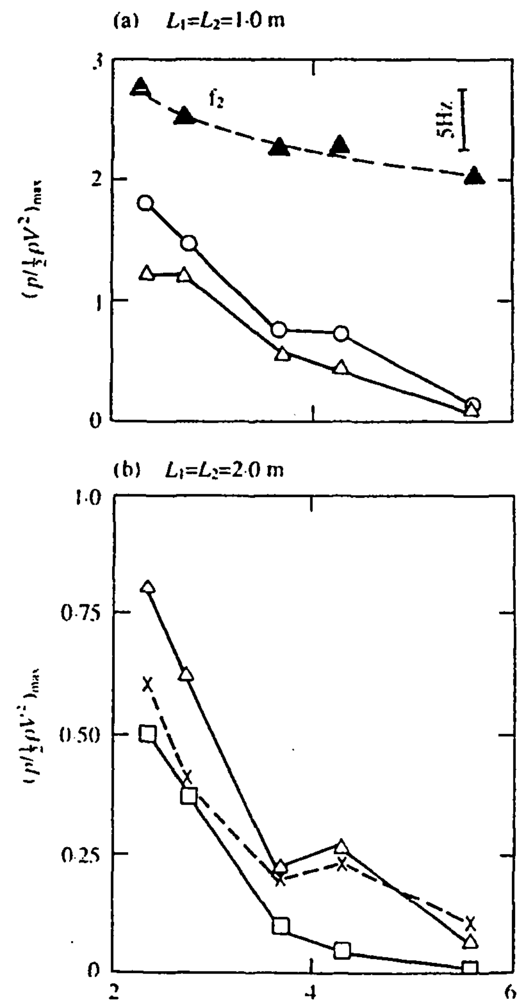

Figure 10. Maximum amplitude measured at the resonance of each mode as a function of the spacing between the tandem branches: (a) $L = 1{\cdot}0$ m; (b) $L = 2{\cdot}0$ m. ○, Mode 1; △, mode 2; □, mode 3; ×, mode 4; ▲, second-mode frequency as a function of l/d. $P_s = 0{\cdot}96$ bar.

The effect of increasing the ratio l/d is twofold: it increases the transmission of the acoustic energy into the main pipe, and therefore increases the damping of the sub-system, and it reduces the intensity of the shear-layer oscillation which excites the system resonance. This can be clarified, in physical terms, by considering the effect of increasing l on the amplitudes of the acoustic pressure and the particle velocity at the mouth of the branches. Since the two branches are acoustically coupled, a pressure minimum (or node) is expected to exist in the main pipe at a distance of $l/2$ from each branch. This expectation is justified since the resonance frequencies decrease with the distance between the branches; see for example the effect of l/d on f_2 which is illustrated in Figure 10(a). Thus, the pressure amplitude at each branch mouth will increase by increasing the distance l (or the ratio l/λ). This increases the transmission of the acoustic energy into the main pipe and therefore, the system resonance is progressively suppressed as the distance l is increased. The other effect of increasing l/d is the reduction of the acoustic particle velocity at the mouth of the branches. Since this particle velocity is the "trigger" of the shear layer oscillation which, in turn, is the energy source sustaining the resonance, the reduction of the particle velocity at the branch mouth is bound to reduce the resonance intensity.

When the distance, l, becomes comparable with half of the acoustic wave length, as in the case of a higher mode for example, a pressure maximum is initiated in the main pipe between the branches as shown in Figure 1(c). Since each branch mouth becomes closer to a pressure minimum, the radiation damping of the sub-system is decreased and the particle velocity exciting the shear layer is increased. This enhances the resonance of the branches again. For the cases $l/d = 4{\cdot}3$ and $5{\cdot}6$, for example, the frequencies corresponding to $l = \lambda/2$ are 780 and 598 Hz, respectively. The higher order modes around these frequencies are seen to be excited in Figures 8(b_1, c_1), but not in Figure 8(a_1) for which the value of l/λ is substantially smaller.

4.3. Tests at High Pressures

Several tests were conducted at higher pressures, to investigate the effect of the fluid density, while keeping other parameters, such as M and S, unchanged. Due to the increase in the fluid density, the maximum flow velocity during the tests was reduced.

The acoustic response of the tandem branches ($L = 1{\cdot}0$ and $2{\cdot}0$ m) and that of the co-axial branches ($L = 0{\cdot}61$ m) at high pressure are compared with those at atmospheric pressure in Figure 11. The first mode of the tandem branches with $L = 2{\cdot}0$ m, Figure 11(a), which was hardly excited at atmospheric pressure is seen to be strongly excited by increasing the fluid density by a factor of about 4. The responses of the other modes also increase, but not as much, by increasing the static pressure.

The increase in the pulsation amplitude, consequent upon increasing the static pressure, is caused by the increase in the fluid density which reduces the acoustic damping due to friction losses and heat conduction at the pipe wall. The effect of increasing the pressure illustrated in Figure 11(c), for example, is indicative of reduced system damping which results in larger amplitudes and wider lock-in range. The influence of fluid density, ρ, on the acoustic damping is given by

$$\alpha = (1/dC)[\mu_e f/4\pi\rho]^{1/2} \qquad \text{(Nepers/m)} \tag{2}$$

where α is the attenuation constant of acoustic waves and μ_e is the equivalent coefficient of viscosity which includes the effect of heat conduction (Kinsler & Frey 1950).

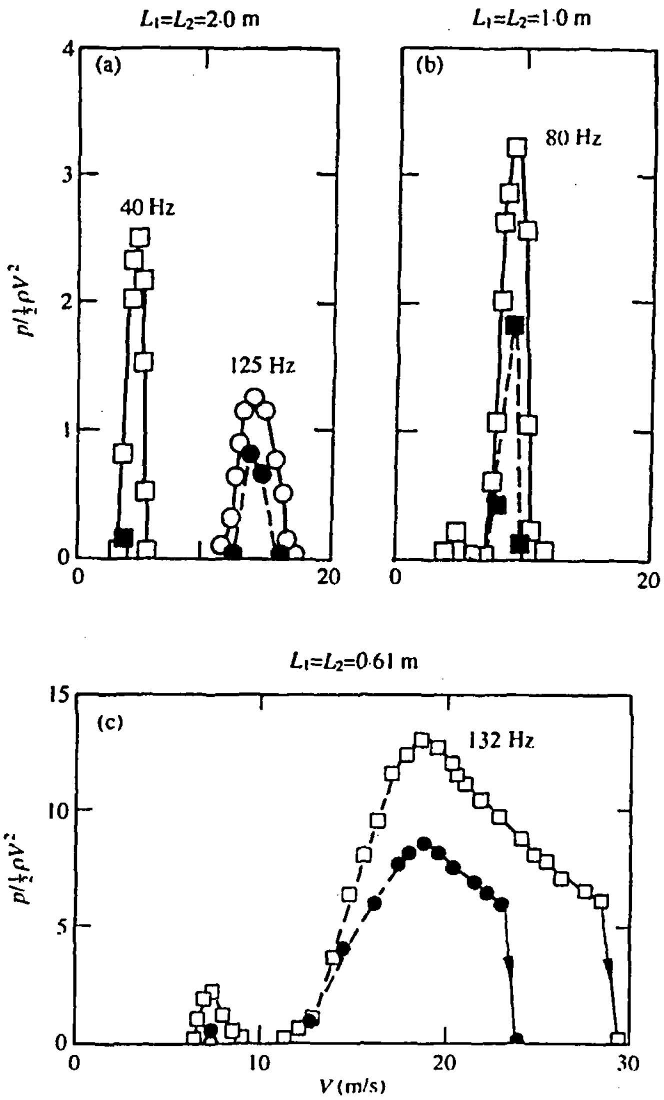

Figure 11. Effect of the static pressure on the pulsation amplitude: (a) and (b) tandem branches, $P_s = 4 \cdot 0$ bar for open data points; (c) co-axial branches, $P_s = 3 \cdot 5$ bar for open data points; $P_s = 0 \cdot 96$ bar for solid data points.

It should be noted, however, that increasing the fluid density also increases the Reynolds number at resonance. Thus, the sharp increase in the response of the first mode shown in Figure 11(a) cannot be attributed to the decrease in the acoustic damping alone but also to the increase in the Reynolds number which was lower than the critical value during the tests at atmospheric pressure.

At relatively high pressures, when the acoustic damping due to friction and heat transfer is negligible, the amplitude of pressure pulsation will be limited due to the sound absorption by the vortex formed at the mouth of the branch. This amplitude-limiting mechanism has been discussed by Bechert (1979), Howe (1980) and Bruggeman (1987) and is referred to in the literature by "vortex damping". At the frictionless limit, Bruggeman *et al.* (1989) have argued that the pulsation amplitude does not scale with $\frac{1}{2}\rho V^2$ but with ρVC, i.e. the acoustic particle velocity at the branch mouth scales with the mean flow velocity in the main pipe. Bruggeman *et al.* estimated, by means of numerical simulation, the critical amplitude at which the sound absorption and production by the vortex balance one another. This critical amplitude is given by

$$(p/\rho VC)_c \simeq 0{\cdot}34 \tag{3}$$

for $S = 0{\cdot}5$ and sharp edges at the branch mouth.

5. COUNTER-MEASURES

5.1. Effect of Detuning the Branches

The resonance frequencies of the branches can be detuned by making one branch shorter (or longer) than the other. This would weaken the acoustic coupling between the branches and therefore the radiation damping of the branches would increase drastically. The effect of making one branch (the downstream one) 15% shorter than the other is shown in Figure 7(a_5, b_5). The data points in these figures represent the r.m.s. amplitudes of the dominant frequency components in the pressure spectra. It is seen that detuning the resonance frequencies is a very effective way of reducing the pulsation amplitude to the level measured for a single branch, Figure 7(a_4, b_4).

However, the detuning process is not as simple as it seems, especially when the branches are relatively long and the operating velocity range is wide, as in the case of turbine by-pass systems. Under these conditions, several resonance modes would be liable to excitation within the velocity range. To avoid the occurrence of large amplitude pulsation, the ratios $\Delta L/L_1$, $\Delta L/l$ and $\Delta L/\lambda$ have to be carefully chosen. This aspect is being investigated further at present.

5.2. Effect of the Spacing Ratio

As mentioned in Section 4.2, the amplitude of the pressure pulsation at the resonance of the lower modes can be reduced by increasing the distance between the branches (l/d). The results of the tests at atmospheric pressure (see Figure 10) show that a value of $l/d = 6$ is sufficiently large in order to avoid large amplitude pulsations. Current tests at higher pressures indicate similar trends, but a relatively larger spacing ($l/d = 10$) is needed to suppress the pressure pulsation adequately. This is due to the fact that the acoustic damping due to friction and heat transfer is lower at higher pressures. Large branch spacings also should be selected with care, to avoid the excitation of a higher order mode when the distance between the branches approaches half the wavelength of an acoustic mode associated with the branches. Bruggeman (1987) reported large amplitude pulsations (14 times the dynamic head) when the branches were separated by a distance of $l \simeq \lambda/2$.

5.3. Effect of the Angle Between the Branches

Several tests were conducted to investigate the case whereby the tandem branches are not in the same plane, i.e. when the branches deviate from the tandem arrangement by an angle θ. The main objective of introducing this angle is to weaken the fluid dynamic coupling between the branches, by reducing the enhancement caused when the vortex formed at the upstream branch arrives at the downstream branch. The tests were carried out in steps of 45°, and at each step the maximum pressure amplitude at

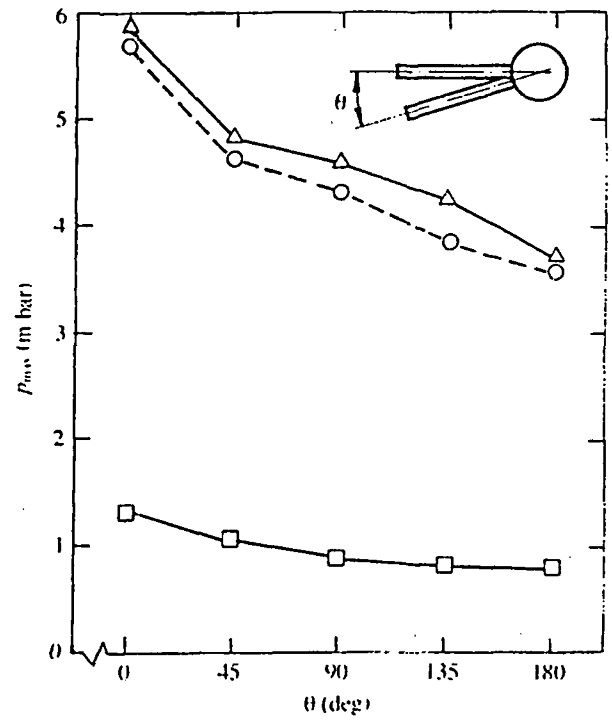

Figure 12. Effect of the angle between the branches on the maximum amplitude measured at resonance, for $l/d = 2{\cdot}75$, $P_s = 4{\cdot}0$ bar: △, $L = 1{\cdot}0$ m, mode 1, 80 Hz; □, $L = 2{\cdot}0$ m, mode 1, 40 Hz; ○, $L = 2{\cdot}0$ m, mode 2, 125 Hz.

resonance was measured. As shown in Figure 12, the resonance amplitude is progressively reduced as the angle θ, is increased. The maximum reduction in the amplitude amounts to 30% at $\theta = 180°$. This amount is clearly insufficient to warrant regarding this design modification as an effective counter-measure.

Since the angle, θ, has virtually no effect on the system acoustic damping, the reduction in the amplitude with the angle θ must be caused by the weakening of the fluid dynamic (or the vortex) coupling between the branches. The effect of this vortex coupling, however, seems to be minor because the reduction in the amplitude with the angle θ, is only slight.

5.4 Effect of the Upstream Turbulence

It is well known that shear layer excitations can be weakened by breaking the two-dimensionality of the flow. This may be achieved by increasing the turbulence level or adding spoilers (often called vortex generators) at the separation point of the shear layer [see, for example, Rockwell & Naudascher (1978), Crighton (1981), Karadogan & Rockwell (1983), Keller & Escudier (1983), Bruggeman (1987) and Ziada *et al.* 1989)]. In order to investigate this possibility, an orifice plate was introduced in the main pipe, to increase the turbulence level in the approach flow. The distance, H, between the orifice plate and the upstream branch was varied, to alter the turbulence level at the mouth of the branches. The area of the orifice was half that of the main pipe. The effect of varying the distance, H, was studied, but no measurements of the turbulence level were carried out.

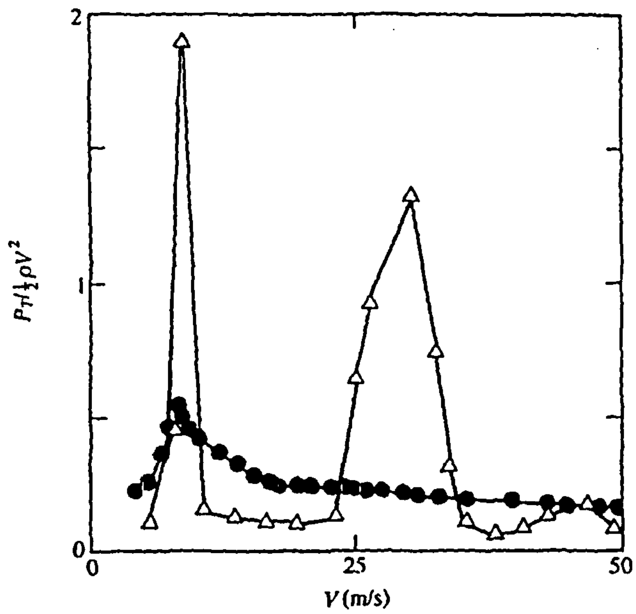

Figure 13. Total r.m.s. amplitude of the pressure pulsation for the case of tandem branches with and without an upstream orifice plate, for $L_1 = L_2 = 1{\cdot}0$ m, $l/d = 2{\cdot}35$, $P_s = 0{\cdot}96$ bar, $H/D = 5{\cdot}5$: Δ, without orifice; ●, with orifice.

As the distance, H, was reduced, the amplitude of the pressure pulsation became smaller, but the resonance peaks became wider. This trend continued until the system response reached its minimum at $H = 5{\cdot}5\,D$. Figure 13 compares this minimum response with the response of the original tandem branches at atmospheric pressure. The data points represent the total r.m.s. amplitude of the pressure pulsation over the frequency range 0 to 1·0 kHz. The resonance amplitudes of the first two modes are seen to be substantially smaller in the presence of the orifice.

As the distance, H, was further reduced to values less than $5{\cdot}5\,D$, the pulsation amplitude started to increase again and the resonance peaks became much wider, i.e. large amplitude pulsations occurred over a wider velocity range. This indicated that the turbulence level produced by the orifice was so high that it excited the system resonances.

The orifice plate was also tested at high pressures. Short co-axial branches ($L = 0{\cdot}61$ m) were chosen for the tests in order to minimize the radiation and friction losses and therefore maximize the amplitude of pressure pulsation. The orifice was positioned at $5{\cdot}5D$ upstream of the branches. Due to the high velocity that was needed to emerge from the lock-in range (30 m/s) and the limited capacity of the facility, it was not possible to increase the static pressure above 3·5 bar.

The results of the tests with and without the orifice plate are given in Figure 14. In the absence of the orifice, the system response shows nonlinear characteristics as exemplified by the occurrence of large amplitude pulsation, the occurrence of a wide range of lock-in and the manifestation of hysteresis effects at the end of the lock-in range. The maximum pulsation amplitude measured during these tests is $p/\rho VC = 0{\cdot}36$. This value agrees very well with the critical amplitude at the frictionless limit ($\approx 0{\cdot}34$) which has been suggested by Bruggeman *et al.* (1989), see Equation (3). Thus, the tested geometry provided rigorous test conditions for the effect of the orifice plate.

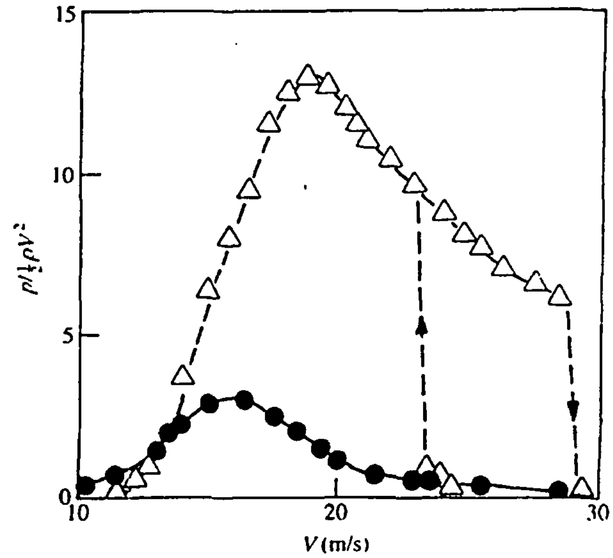

Figure 14. Amplitude of the pressure pulsation for the case of co-axial branches with and without an upstream orifice plate, for $L_1 = L_2 = 0{\cdot}61$ m, $P_s = 3{\cdot}5$ bar, $H/D = 5{\cdot}5$: △, without orifice; ●, with orifice.

As indicated in Figure 14, the orifice plate reduces the amplitude of the pressure pulsation substantially.

It should be noted that Bruggemann (1987) investigated the effect of spoilers which were positioned at one diameter upstream of two side-branches. He found that the spoilers became less effective when the test pressure was increased. This may be attributed to the smallness of the length scale of the turbulence generated by the spoilers; the spoiler size was about $\frac{1}{10}$th the vortex size. In the present tests, the turbulence scale is comparable with the size of the vortex formed at the branch mouth and therefore the orifice plate may be more effective at high pressures than the spoilers. Irrespective of this difference, the findings of Bruggeman underline the need to be cautious when applying the present results to cases involving higher pressures than those tested in this study.

The reduction in the amplitude caused by the orifice plate is not related to any alteration in the system acoustic damping. The orifice plate is positioned in the main pipe in which the amplitude of the pressure pulsation is very small: about 50 times smaller than that in the branches. At such low amplitudes, sound absorption by orifice plates is negligible (Ingard 1967). In addition, the area ratio of the orifice (0·5) is too large to cause any considerable change in the acoustic characteristics of the system, even in the presence of flow.

In summary, the use of an orifice plate upstream of the branches can substantially reduce the intensity of the system resonances. The orifice plate, however, should not be positioned too close to the branches, otherwise the turbulence generated by the orifice may become an excitation source in itself. A distance of 5·5 D was found to be an optimum distance in the present tests.

5.5. Additional Counter-Measures

Several other counter-measures which have been reported in the literature are very noteworthy. Jungowski & Studzinski (1989) developed an insert which can be placed at the mouth of side-branches. They were able to suppress the pressure pulsation by a factor of 100 in some cases. This superior counter-measure deserves further attention to confirm its performance in cases involving multiple side-branches with a large diameter ratio and operating at high pressures. Bruggeman (1987) has also tested several counter-measures. Most effective was the addition of spoilers (or a plate) at the upstream edge of the downstream branch.

All the counter-measures discussed in this paper reduce the pressure pulsation to varying degrees. A successful solution to a problem may require the adoption of more than one counter-measure. The designer should at first evaluate the side effects which may arise from the adoption of any of these counter-measures. For example, a design modification which suppresses the pressure pulsations when the side-branches are closed, may cause other problems when the flow is diverted into the branches.

6. SUMMARY AND CONCLUSIONS

Flow-induced acoustic resonances of two side-branches in close proximity have been investigated experimentally. The resonance of the two branches is found to be much stronger than that of a single branch under similar test conditions. This difference is caused by the acoustic coupling between the two branches which drastically reduces the acoustic radiation into the main pipe. Co-axial branches produce the strongest resonance because their radiation damping is minimal. Pulsation amplitudes up to 13 times the dynamic head in the main pipe have been recorded. This value is about two orders of magnitude higher than that observed in the case of a single branch under the same test conditions.

Several tests have been carried out to investigate the effect of the geometrical and flow parameters on the general acoustic response of the system. The main findings of these tests are summarized in the following.

(i) The acoustic modes of the branch subsystem are excited consecutively, as the flow velocity in the main pipe is increased. The resonances occur in the main within a Strouhal number range of 0·27 to 0·55. Resonances can also occur at a higher Strouhal number ($S \simeq 0{\cdot}9$), but these resonances are much weaker than those occurring within the main Strouhal number range.

(ii) In all tests, the Strouhal number for large amplitude pulsations did not exceed 0·55. Acoustic resonances can therefore be avoided by keeping the Strouhal number, based on the first mode frequency and the maximum flow velocity, higher than 0·55.

(iii) The dimensionless amplitude at resonance increases as the static pressure is increased. This is due to the reduction in the acoustic damping due to friction at higher pressures.

(iv) The dimensionless amplitude at the resonance of the higher modes decreases continually as the mode order is increased.

(v) Resonances become progressively weaker as the distance between the branches is increased.

(vi) The angle θ between the branches has only a minor effect on system response. The pulsation amplitude decreases slightly as the angle between the branches is increased.

(vii) De-tuning the resonance frequencies of the branches, by making the branches be of different lengths, is the most effective counter-measure.

(viii) Increasing the turbulence level of the approach flow considerably reduces the pulsation amplitude. This attenuation effect vanishes as the turbulence level exceeds a certain limit and itself becomes an excitation source.

The present study dealt with a single diameter ratio ($d/D = 0{\cdot}57$). We expect similar trends for larger diameter ratios. For smaller diameter ratios, however, the difference between single and multiple side-branches is expected to become progressively smaller as the diameter ratio is decreased. Finally, it should be made clear that the present study does not suggest in anyway that single side-branches do not produce large amplitude pressure pulsations. It shows rather that multiple side-branches with large diameter ratios can cause serious problems, although a similar single branch may not cause any problem under the same conditions.

ACKNOWLEDGEMENTS

The work described in this paper forms part of the research project: Flow-Excited Resonances in Complex Pipe Systems. This project is jointly supported by "Nationaler Energie-Forschungs-Fonds" (NEFF) and Sulzer Brothers Limited. The authors are grateful to Messrs A. Foude, R. Qian and M. El-Shazly for conducting some exploratory experiments during the initial period of the project.

REFERENCES

BALDWIN, R. M. & SIMMONS, H. R. 1986 Flow-induced vibration in safety relief valves. *ASME Journal of Pressure Vessel Technology* **108**, 267–272.

BECHERT, D. W. 1979 Sound absorption caused by vorticity shedding, demonstrated with a jet flow. American Institute of Aeronautics and Astronautics, Paper AIAA 79-0575.

BERNSTEIN, M. & BLOOMFIELD, W. 1989 Malfunction of safety valves due to flow-induced vibrations. In *Flow-Induced Vibrations–1989,* AMSE Publication No. 154 (eds M. K. Au-Yang, S. S. Chen, S. Kaneko and R. Chilukuri), pp. 155–164. New York: ASME.

BRUGGEMAN, J. C. 1987 Flow-induced pulsations in pipe systems. Doctoral Dissertation. Technische Universität Eindhoven, Eindhoven, The Netherlands.

BRUGGEMAN, J. C., HIRSCHBERG, A., VAN DONGEN, M. E. H., WIJNANDS, A. P. J. & GORTER, J. 1989 Flow induced pulsations in gas transport systems: Analysis of the influence of closed side branches. *ASME Journal of Fluids Engineering* **111**, 484–491.

CHEN, Y. N. & FLORJANCIC, D. 1975 Vortex-induced resonance in a pipe system due to branching. International Conference on Vibration and Noise in Pumps, Fan and Compressor Installations, University of Southampton, England, pp. 79–86.

CHEN, Y. N. & STUERCHLER, R. 1977 Flow-induced vibrations and noise in a pipe system with blind branches due to coupling of vortex shedding. *Internoise* **77**, Zürich, B189–B203.

CHEN, Y. N. & ZIADA, S. 1982 Strömungserregte Schwingungen infolge Wirbelkopplung in der HZUE-Leitung. Sulzer Brothers Limited, Report No. 1512/2803.

COFFMAN, J. T. & BERNSTEIN, M. D. 1980 Failure of safety valves due to flow-induced vibration. *ASME Journal of Pressure Vessel Technology* **102**, 112–118.

CRIGHTON, D. G. 1981 Acoustics as a branch of fluid mechanics. *Journal of Fluid Mechanics* **106**, 261–298.

DE METZ, F. C. & FARABEE, T. M. 1977 Laminar and turbulent shear flow induced cavity resonances. American Institute of Aeronautics and Astronautics, Paper No. AIAA 77-1293.

EAST, L. F. 1966 Aerodynamic induced resonances in rectangular cavities. *Journal of Sound and Vibration* **3**, 227–287.

ELDER, S. A. 1978 Self-excited depth-mode resonance for a wall-mounted cavity. *Journal of the Acoustical Society of America* **64**, 877–890.

ELDER, S. A., FARABEE, T. M. & DE METZ, F. C. 1982 Mechanisms of flow-excited cavity tones at low Mach number. *Journal of the Acoustical Society of America* **72**, 532–549.

ERICKSON, D. D., DURGIN, W. W., MAGUIRE, C. F. & MOELLER, M. 1986 Shear layer coupling with side-branch resonators. *Forum on Unsteady Flow,* ASME Publication No. FED 39, pp. 43–45.

HOURIGAN, K., STOKES, A. N., THOMPSON, M. C. & WELSH, M. C. 1986 Flow-induced acoustic resonances for a bluff body in a duct: a numerical study. In *Proceedings 9th Australasian Fluid Mechanics Conference*, Auckland, pp. 504–507.

HOURIGAN, K., WELSH, M. C., THOMPSON, M. C. & STOKES, A. N. 1990 Aerodynamic sources of acoustic resonances in a duct with buffles. *Journal of Fluids and Structures* **4**, 345–370.

HOWE, M. S. 1975 Contributions to the theory of aerodynamic sound, with application to excess jet noise and the theory of the flute. *Journal of Fluid Mechanics* **71**, 625–673.

INGARD, U. 1967 Acoustic nonlinearity of an orifice. *Journal of the Acoustical Society of America* **42**, 6–17.

JUNGOWSKI, W. M., BOTROS, K. K. & STUDZINSKI, W. 1989 Cylindrical side-branch as tone generator. *Journal of Sound and Vibration* **131**, 265–285.

KARADOGAN, H. & ROCKWELL, D. 1983 Toward attenuation of self-sustained oscillations of a turbulent jet through a cavity. *ASME Journal of Fluid Engineering* **105**, 335–339.

KELLER, J. J. & ESCUDIER, M. P. 1983 Flow excited resonances in covered cavities. *Journal of Sound and Vibration* **86**, 199–226.

KINSLER, L. E. & FREY, A. R. 1950 *Fundamentals of Acoustics*, p. 240. New York, John Wiley and Sons.

PARTHASARATHY, S. P., CHO, Y. I. & BACK, L. H. 1985 Sound generation by flow over relatively deep cylindrical cavities. *Journal of the Acoustical Society of America* **78**, 1785–1795.

ROCKWELL, D. 1979 Self-sustained oscillations of impinging free shear layers. *Annual Reviews of Fluid Mechanics* **11**, 67–94.

ROCKWELL, D. 1983 Oscillations of impinging shear layers. *American Institute of Aeronautics and Astronautics Journal* **21**, 645–664.

ROCKWELL, D. & NAUDASCHER, E. 1978 Review—Self-sustaining oscillations of flow past cavities. *ASME Journal of Fluids Engineering* **100**, 152–165.

STONEMAN, S. A. T., HOURIGAN, K., STOKES, A. N. & WELSH, M. C. 1988 Resonant sound caused by flow past two plates in tandem in a duct. *Journal of Fluid Mechanics* **192**, 455–484.

ZIADA, S., BUEHLMANN, E. T. & BOLLETER, U. 1989 Flow impingement as an excitation source in control valves. *Journal of Fluids and Structures* **3**, 529–549.

APPENDIX: NOMENCLATURE

C	speed of sound
D	diameter of the main pipe
d	diameter of the branch pipe
f_n	frequency of acoustic mode, n
H	distance between orifice and upstream branch
L_1, L_2	branch length
l	distance between branches
ΔL	$L_1 - L_2$
M	Mach number, V/C
n	order of acoustic mode
P_T	total r.m.s. amplitude of pressure pulsation
p	r.m.s. amplitude at the resonance frequency
p_{max}	maximum amplitude reached at resonance
P_s	absolute static pressure in the main pipe
R	Reynolds number, $\rho VD/\mu$
r	edge radius at the branch mouth
S	Strouhal number, $S = fd/V$
V	flow velocity in the main pipe
α	attenuation constant of acoustic wave in pipes
θ	angle between branch pipes
λ	acoustic wavelength
μ	dynamic viscosity
ρ	density of the flowing medium